Journal of the Serbian Chemical Society
JSCS-info@shd.org.rs • www.shd.org.rs/JSCS
J. Serb. Chem. Soc. 77 (2) 211–224 (2012)
JSCS–4262
UDC 547.478+546.11+544.35:542.8
Original scientific paper

On the kinetics of the hydrogen evolution reaction on Ni–MoO_x composite catalysts in alkaline solutions

BORKA M. JOVIĆ[1], UROŠ Č. LAČNJEVAC[1#], VLADIMIR D. JOVIĆ[1], LJILJANA M. GAJIĆ-KRSTAJIĆ[2#] and NEDELJKO V. KRSTAJIĆ[3]

[1]Institute for Multidisciplinary Research, University of Belgrade, P. O. Box 33, 11030 Belgrade, Serbia, [2]Institute of Technical Sciences SASA, Knez Mihajlova 35, 11000 Belgrade, Serbia and [3]Faculty of Technology and Metallurgy, University of Belgrade, Karnegijeva 4, 11000 Belgrade, Serbia

(Received 21 June, revised 19 September 2011)

Abstract: MoO_3 particles were co-deposited with Ni onto smooth or rough Ni supports from modified Watt baths of different compositions. Morphology and composition of the electrodeposits were characterized by means of cyclic voltammetry, X-ray diffraction analysis, scanning electron microscopy, transmission electron microscopy and energy dispersive X-ray spectroscopy. The electrocatalytic activity of the composite catalysts for H_2 evolution in alkaline solutions was determined by quasi-stationary polarization curves. Activity increases with MoO_x content in the Ni deposit up to a limiting value. The composite Ni–MoO_x catalysts exhibited high catalytic activity, similar to that of a commercial Ni–RuO_2 catalyst. Stability tests showed that the Ni–MoO_x co-deposits were stable under constant current conditions and exhibited excellent tolerance to repeated short-circuiting.

Keywords: hydrogen evolution; nickel; molybdenum trioxide; composite catalyst; co-deposition.

INTRODUCTION

The hydrogen evolution reaction (HER) is one of the most studied electrochemical reactions because it occurs through a limited number of reaction steps with only one reaction intermediate involved. It is a unique electrochemical reaction for which the complete theory of electrocatalysis was developed.[1,2]

Hydrogen evolution is the most frequent cathodic reaction in industrial electrolytic processes and has been recognized as a valuable fuel that may well replace oil as an energy source. It also plays a major role in synthetic organic chemistry in the well-known catalytic hydrogenation process.[3] One major aspect of

* Corresponding author. E-mail: nedeljko@tmf.bg.ac.rs
# Serbian Chemical Society member.
doi: 10.2298/JSC112106185J

the research undertaken is to improve catalytic electrode materials in terms of their activity, efficiency and mechanical and corrosion stability. Nickel-based materials were shown to exhibit these characteristics and are widely used in industrial processes.

Alloying two metals has long appeared to be the most straightforward way of achieving electrocatalytic activation. In the case of the hydrogen evolution reaction, it seems that Ni–Mo catalysts, either electrodeposited,[4] or thermally prepared,[5] or added *in situ*,[6] have constituted the main objective of research during the past twenty years.

Synergetic effects were explicitly ruled out in the case of *in situ* activation with molybdate.[7,8] As molybdate was deposited from technical solutions, a co-deposit of Mo and Ni (Fe, Co) was in fact formed, but the Tafel slope remained the same as that for pure Ni. The same was the case of Ni–Mo bulk alloys.[9] In the case of Ni–Mo catalysts prepared by thermal decomposition of suitable precursors, synergetic effects were observed, with a maximum at around 30 at. % Ni.[10] The Tafel slope decreased to 40 mV and extended to very high current densities, while the exchange current density close to 10 mA cm^{-2} was by three orders of magnitude higher than that for bulk Ni. However, these electrodes did not possess the expected stability during prolonged electrolysis, mainly due to the drastic irreversible reduction of the corresponding metal oxides during cathodic polarization, which caused the collapse of the oxide lattice.[11]

Ni–Mo coatings obtained by electroplating exhibited so-called "synergetic effects" in contrast to Ni–Mo bulk alloys.[12,13] The specific role of Mo in Ni–Mo electroplated coatings could be explained by the fact that the molybdenum was present more likely as an amorphous oxides phase than as a pure metallic phase. However, the morphology of Ni (Fe,Co)–Mo electroplated coatings were characterized by the presence of numerous micro-cracks down to the support.[14–18] Accumulation of molecular hydrogen in localized areas, such as micro-cracks, in the coating may result in the formation of internal bursts or blisters and the coating becomes mechanically fragile. In addition, it was found that Mo is not at all stable in alkaline solution when a cell is shut down, as it tends to be leached out, which could be the origin of deactivation on cathodic load.[19]

Improved performances are to be expected if a composite compact layer of Ni and some Mo oxides could be prepared by the simultaneous electrodeposition of Ni and MoO_3 from an electrolyte solution in which MoO_3 particles are suspended. It seems a unique way for solving the problem of porosity of electroplated Ni–Mo coatings and low mechanical stability of thermally prepared Ni–Mo catalysts. Therefore, the aim of this study was to determine the conditions for the preparation of compact Ni–MoO_x composite coatings possessing high catalytic activity towards the HER.

EXPERIMENTAL

Electrode preparation

The Ni/(Ni–MoO_x) active cathodes were prepared by the simultaneous electrodeposition of Ni and suspended MoO_3 particles onto a Ni substrate from a Watt bath of the following composition: $NiSO_4 \cdot 6H_2O$ – 330 g dm^{-3}; $NiCl_2 \cdot 6H_2O$ – 45 g dm^{-3}; H_3BO_3 – 38 g dm^{-3}; pH: 3.2–4.0. The deposition was performed at 40 °C. Nickel platelets (10 mm×10 mm×0.2 mm) with a very thin stem were used as substrates.

The MoO_3 powder was prepared by thermal decomposition of $(NH_4)_6Mo_7O_{24} \cdot 4H_2O$ at 500 °C for 2 h under an air atmosphere[20] and was dispersed by means of a magnetic stirrer. The amount of MoO_3 particles in the bath was varied between 0 and 20 g dm^{-3}.

The pre-treatment of the Ni support consisted of either etching (HCl) or mechanical polishing (emery paper). Electrodeposition was performed galvanostatically in a stirred solution (magnetic stirrer at 400 rpm) at 40 °C by varying the current density, typically from 5 to 50 mA cm^{-2}, for a constant electricity (72 C cm^{-2}). All deposition experiments were performed using a self-made rectifier.

Electrode characterization

Scanning electron microscopy (SEM, on JOEL 840) was used to characterize the morphology of the as-deposited surface. Transmission electron microscopy (TEM) measurements were performed using the FEI (Fillips Electronic Instruments) – CM200 super-twin and CM300 ultra-twin microscopes operating at 200 and 300 kV, equipped with Gatan 1k×1k and 2k×2k CCD cameras, respectively. Specimens for TEM analysis were prepared by making a suspension of the catalyst powder in ethanol, using an ultrasonic bath. The catalyst powder was prepared by grounding the Ni–MoO_x coating electrodeposited onto a glassy carbon support. XRD Analysis of Ni–MoO_3 composite coatings was carried out by Siemens D-500 diffractometer. CuK radiation was used in conjunction with a CuK (nickel filter). Obtained X-ray diffraction pattern was used to evaluate the phase structure and crystallite size of the coatings.

Cell and chemicals

A conventional three-compartment cell was used. The working electrode (WE) compartment was separated by fritted glass discs from the other two compartments. The WE compartment was jacketed and thermostated during measurements at 25.0 °C or at 85 °C, using a thermostat. All measurements were performed in 1.0 mol dm^{-3} or 33 wt. % NaOH solution (Spectrograde, Merck), prepared in deionized water. The WE compartment was saturated with purified hydrogen at standard pressure during measurements. A saturated calomel electrode (SCE) or a reversible hydrogen electrode (RHE) in the same solution were used as the reference electrodes while a flat Pt sheet served as the counter electrode.

Electrochemical measurements

Tafel lines were recorded using potentiostatic steady-state voltammetry, point by point at 60 s intervals, using a PAR 273 potentiostat, with good reproducibility of measurement. Whenever the potential of the WE approached approximately –1.3 V (SCE) (or when current densities were close to, above approximately 0.1 A cm^{-2}) it was found that the uncompensated solution resistance (IR drop) was significant. Therefore, the IR drop was systematically determined in all measurements, using ac impedance methods. All data presented in this report are corrected for the IR drop.

RESULTS AND DISCUSSION

Efficiency of electrodeposition

The variation of the current efficiency for Ni electrodeposition as a function of the concentration of MoO_3 particles in the solution at a constant current density of 10 mA cm^{-2} is shown in Fig. 1. The current efficiency was estimated from deposition charge and weight increase measurements, assuming that the latter was due to Ni only, without correction for the contribution to the overall weight increase of the dispersed phase. As can be seen from Fig. 1, the current efficiency did not depend significantly on the concentration of suspended MoO_3 particles in the range from 1 to 20 g dm^{-3}. The current efficiency for Ni electrodeposition was generally very low, indicating a high catalytic activity of the Ni–MoO_x co-deposits for the HER, which occurred as a parallel reaction during electrodeposition. However, it is important to emphasize that partial reduction of MoO_3 can also takes place during electrodeposition, according to the following overall reactions:

$$MO_3 + xH^+ + xe \rightleftarrows H_xMoO_3 \quad (1)$$

or

$$MO_3 + 2yH^+ + 2ye \rightleftarrows MoO_{3-y} + yH_2O \quad (0<y<1) \quad (2)$$

Reaction (1) or (2) could additionally reduce the current efficiency for Ni electrodeposition.

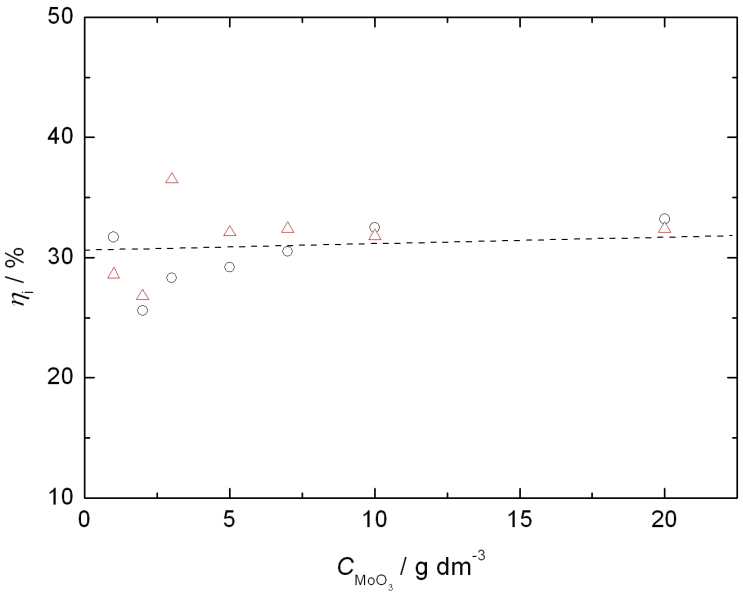

Fig. 1. Effect of the MoO_3 content in the Watt bath on the current efficiency of Ni+MoO_3 co-deposition at j_{Ni} = 10 mA cm^{-2} (circles and triangles present two different measurements).

This speculation is based on previous experiments that showed the reduction of MoO_3 powder in a hydrogen atmosphere at temperature of 623 K proceeded *via* the formation of hydrogen molybdenum bronze, H_xMoO_3. Therefore, during Ni+MoO_3 co-deposition, the formation of similar reduced phases of MoO_3 could occur in which hydrogen species adsorbed onto the Ni surface participate in this reaction.

The dependence of the current efficiency on the applied current density of deposition at a constant concentration of suspended MoO_3 particles in the bath (1 g dm^{-3}) is shown in Fig. 2. The current efficiency decreases with increasing applied current density, probably due to the increase in the relative deposition rate of Ni to MoO_3 particles, which leads to an increase of the catalytic activity of composite (Ni–MoO_x) coatings for the HER.

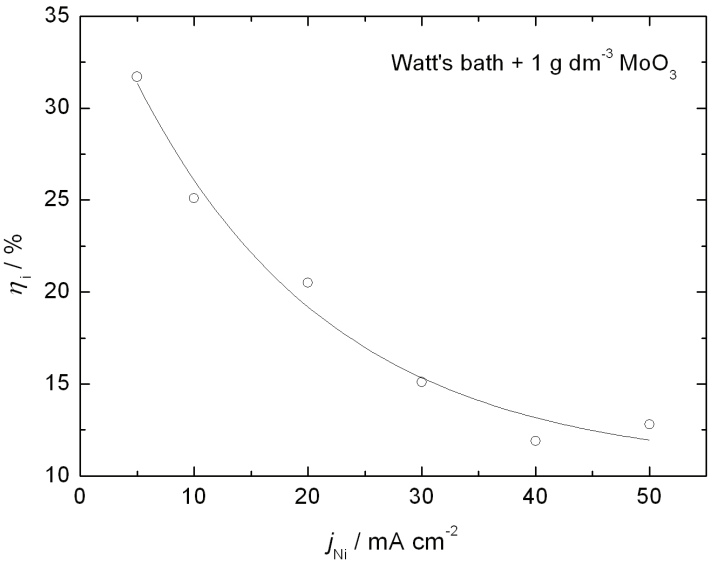

Fig. 2. Current efficiency for Ni+MoO_3 co-deposition as a function of the applied current, determined in a Watt bath containing 1 g dm^{-3} of MoO_3 particles.

Morphology and chemical composition of composite the Ni–MoO_x electrodeposits

Typical top views of the Ni–MoO_x composites electrodeposited at different current densities from a Watt bath containing 1 g dm^{-3} of suspended particles MoO_3. As can be seen, the morphology of the Ni–MoO_x coating deposited at a lower current density is characterized by the presence of micro-cracks, with some 2 μm in width (Fig. 3a), and a high concentration of MoO_3 particles. However, the electrodeposit formed at a higher current density is microcrystalline and compact (Fig. 3c).

The X-ray diffraction (XRD) pattern for a Ni–MoO_x electrodeposit is shown in Fig. 4. It was found that the XRD peaks of MoO_3 had disappeared after co-deposition with Ni and that the Ni–MoO_x composite coating was completely amorphous in nature. The reason for the disappearance of the corresponding XRD peaks is not clear at this stage; the change to an amorphous MoO_x phase during the co-deposition is probably the result of a reduction process in which H_{ads} species participate. Thus, due to amorphous nature of the coating, it was necessary to characterize the composite coating by energy dispersive X-ray spectroscopy (EDS) to determine the chemical composition of the Ni–MoO_x coatings.

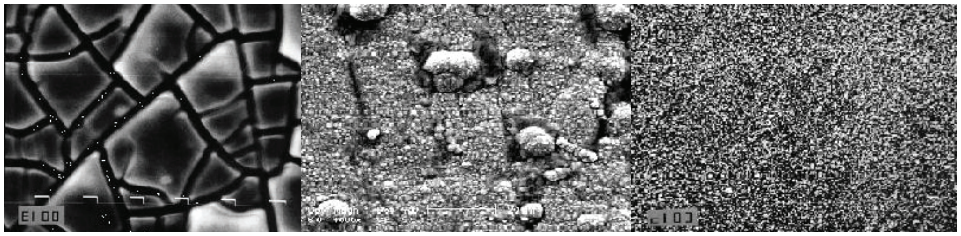

(a) (b) (c)

Fig. 3. Scanning electron micrographs of the Ni–MoO_x electrode surfaces electrodeposited at: a) j_{Ni} = 10 mA cm^{-2}; b) j_{Ni} = 20 mA cm^{-2}; c) j_{Ni} = 50 mA cm^{-2}. The concentration of MoO_3 particles in the Watt bath was 1 g dm^{-3}. Magnification 1000×.

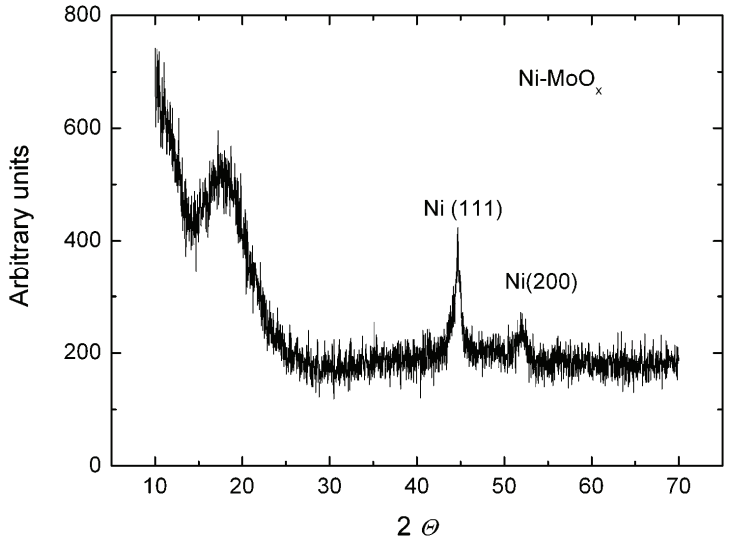

Fig. 4. XRD Pattern (2Θ in degrees) of the composite (Ni–MoO_x) coating prepared by electrodeposition from a Watt bath containing 1 g dm^{-3} of MoO_3 particles at j_{Ni} = 10 mA cm^{-2}.

The amount of MoO_x could hardly be determined by surface spectroscopies, because of the localization of the MoO_x particles, but TEM analysis showed that

MoO_x particles (white spots) were relatively uniformly distributed in Ni matrices (Fig. 5). The chemical composition of the coating (sample obtained by electrodeposition at 30 mA cm^{-2}) at different positions (EDS spectra) is presented in Fig. 5.

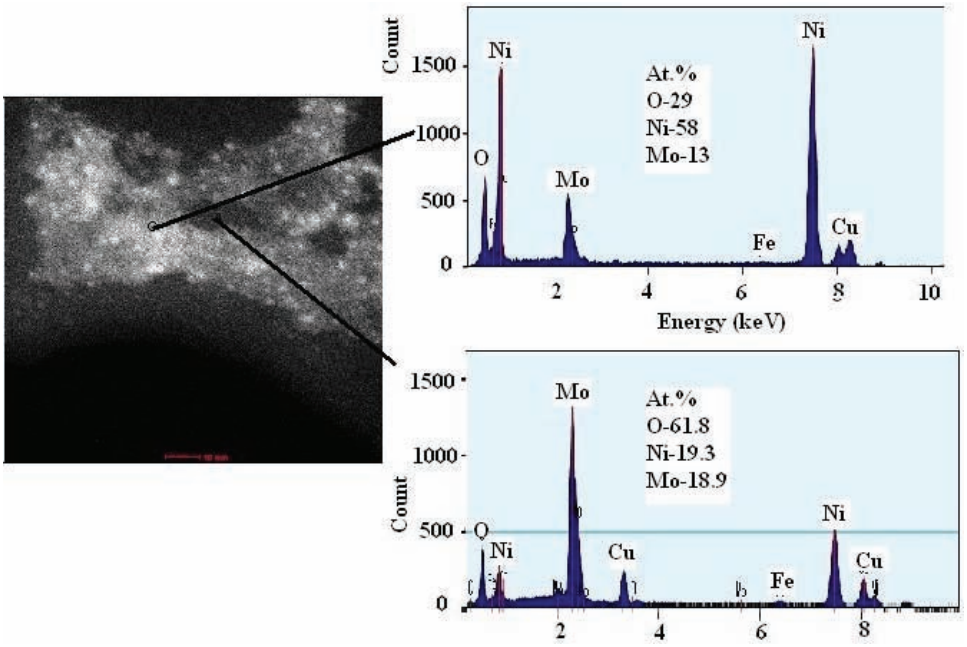

Fig. 5. TEM dark field image and EDS spectra of an electrodeposited Ni–MoO_x layer (j_{Ni} = 50 mA cm^{-2}; 1 g dm^{-3} MoO_3) on a smooth Ni support from a Watt bath. The MoO_x particles are presented by white spots and the corresponding EDS spectra of the region with a low and a high content of Mo oxides.

The average content of Mo oxides in the composite coating generally decreased with increasing deposition current density.

Cyclic voltammetry in 1.0 mol dm^{-3} NaOH

The electrode surfaces of the Ni–MoO_x catalysts were characterized by means of their voltammetric curves (VC). A series of VCs recorded at different scan rates is shown in Fig. 6. The corresponding curves of Ni in the same solution are shown in Fig. 7, for comparison. Reproducible and characteristic voltammograms were obtained. Both electrodes are characterized by a highly reversible peak prior to the oxygen evolution reaction. The reactions occurring at potentials in the range of both the anodic current and the cathodic current peaks are apparently complementary processes, which are represented by the overall reaction:

$$\mathrm{NiO(hydrated)} + \mathrm{OH^-} \rightleftarrows \mathrm{NiOOH} + e^- \quad (3)$$

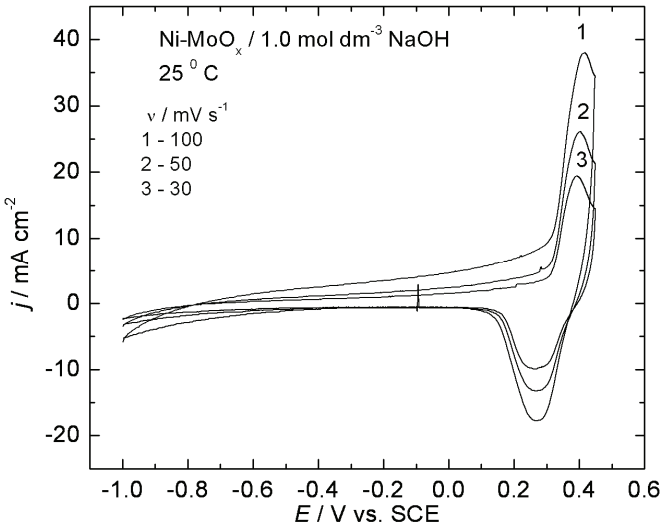

Fig. 6. Cyclic voltammetric curves over the potential range of –1.0 to 0.45 V (SCE) of a Ni/(Ni–MoO_) composite electrode (prepared by electroplating at 50 mA cm^{-2} in a Watt bath containing 1 g dm^{-3} of MoO_3 particles) in 1.0 mol dm^{-3} NaOH solution at 25 °C.

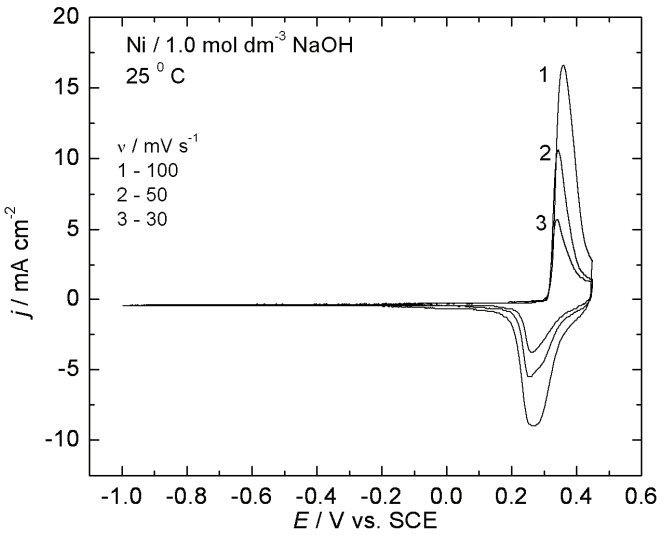

Fig. 7. Cyclic voltammetric curves over the potential range –1.0 to 0.45 V (SCE) of a Ni electrode in 1.0 mol dm^{-3} NaOH solution.

The anodic and cathodic processes referred to in Eq. (3) are highly reversible, in which the solid-state diffusion of hydroxide ions is the rate determining step. It is interesting to emphasize that the introduction of MoO_3 particles into the Ni deposit increased the peak of NiO oxidation and shifted it towards a more

positive value (≈ 50 mV). Consistently, O_2 evolution commenced at a *ca.* 50 mV more negative potential on the Ni electrode than on the composite. The increase of both the anodic and cathodic peaks could be explained by the surface of Ni–MoO_x being rougher than that of the etched Ni surface, because the participation of Mo oxides redox reactions could not be expected, according to the thermodynamic data. Anodic peak current density of the Ni–MoO_x composite catalyst was around two times higher, which means that the real surface area of this electrode is approximately two times higher than the real surface area of the etched Ni electrode.

Polarization measurements in 1.0 mol dm^{-3} NaOH

The polarization curves for the HER obtained on different Ni/(Ni–MoO_x) electrodes prepared by co-deposition onto a mechanically polished Ni substrate, from 1.0 mol dm^{-3} NaOH solution are shown in Fig. 8. The polarization curves were recorded after holding the electrodes at a constant cathodic current density of 100 mA cm^{-2} for about 1 h. The polarization curves are characterized by two Tafel slopes at all electrodes, $b_1 \approx -40$ mV in the lower overpotential region and $b_2 \approx -120$ mV in the high overpotential region. The composite Ni–MoO_x coating obtained by electroplating at j_{Ni} = 50 mA cm^{-2} was found to have the lowest hydrogen overpotential (Fig. 9) and the highest exchange current density, $j_0 \approx$ ≈ 7.9×10^{-4} A cm^{-2} (Fig. 8). The corresponding kinetic parameters for the HER for these electrodes are presented in Table I.

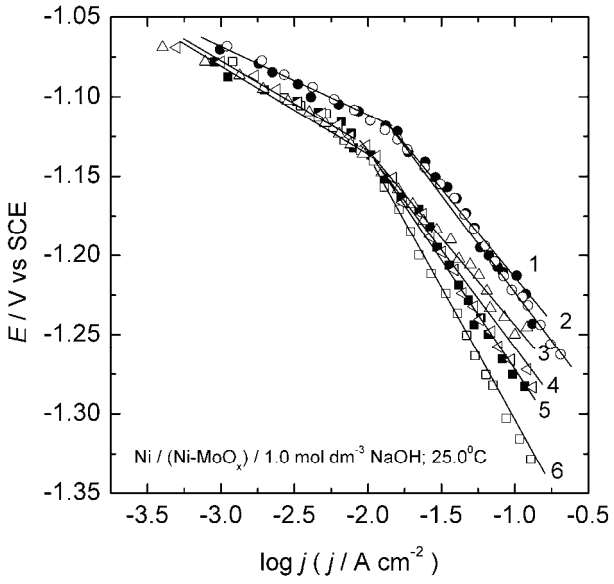

Fig. 8. Tafel polarization curves for the HER on Ni/(Ni–MoO_x) electrodes in 1.0 mol dm^{-3} NaOH solution at 25 °C. The electrodes were prepared by electrodeposition from a Watt bath containing 1.0 g dm^{-3} of MoO_3 particles at different current densities (mA cm^{-2}): 1) 50; 2) 40; 3) 30; 4) 20; 5) 10; 6) 5.

Typical polarization curves for the HER on polished Ni and the most active Ni/(Ni–MoO_x) electrode are shown in Fig. 10, for comparison. In contrast to Ni/

/(Ni–MoO_x), only one Tafel slope of about –120 mV dec^{-1} is present over the complete potential range for the HER on Ni. At the same potential, the activity of Ni/(Ni–MoO_x) was about four orders of magnitude higher than that of the Ni electrode. It is clear from the morphological investigations that the incorporation of MoO_3 particles into a Ni deposit produces roughness, but undoubtedly, syner-

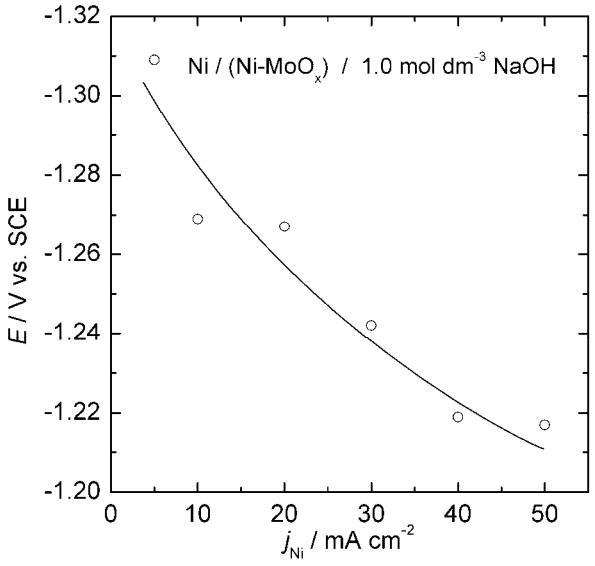

Fig. 9. Potential for the HER at j_{H_2} = 100 mA cm^{-2} on Ni/(Ni–MoO_x) composite electrodes in 1.0 mol dm^{-3} NaOH, prepared by electroplating at different current densities.

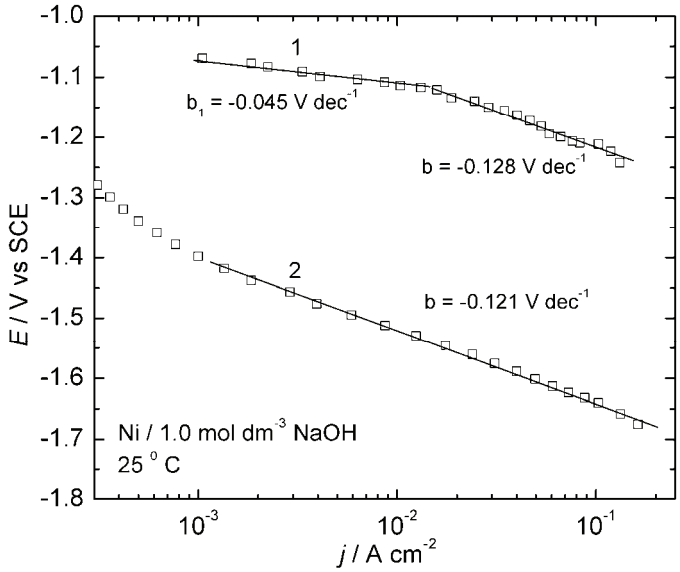

Fig. 10. Tafel polarization curves for the HER on the most active Ni/(Ni–MoO_x) electrode (electrode 1 from Fig. 8) and on an etched Ni electrode in 1.0 mol dm^{-3} NaOH solution at 25 °C.

getic effects are achieved, because the Tafel slope decreases to –40 mV in the lower overpotential region and extends to relatively high current densities. It was shown[21] that the reaction mechanism of the HER on Ni is a consecutive combination of a Volmer and a Heyrovsky step, and that the Heyrovsky step prevails over the Tafel step in the low overpotential region and that the reaction rate is controlled by the Heyrovsky reaction with an almost full coverage by $H_{ads.}$ However, the presence of Tafel slope of –40 mV for the HER on the Ni/(Ni–MoO_x) electrode indicates that the Heyrovsky step controls the rate of the overall reaction in the lower potential range, but with a low coverage by H_{ads} intermediates. In accordance with the mechanism of the HER, both the Volmer and the Heyrovsky steps occurred at a single adsorption site and the reaction occurred at the Ni electrode with an almost full coverage by H_{ads}, but with a low coverage by H_{ads} in the case of the Ni/(Ni–MoO_x) electrode. The fact that the reaction rate was almost four orders of magnitude higher on the latter electrode, indicates an increased catalytic activity of the adsorption sites for the HER on the Ni/(Ni––MoO_x) electrode.

Electrochemical characteristics of the composite Ni–MoOx catalyst in 33 wt.% NaOH solution

The polarization characteristics of the most active Ni/(Ni–MoO_x) cathode were tested in a 33 wt. % NaOH solution at 85 °C, which are typical conditions for industrial chlor–alkali electrolysis.

The polarization curve for the HER at the Ni/(Ni–MoO_x) electrode is shown in Fig. 11. The polarization curve for the HER at a commercial DN3 electrode (Ni–RuO_2, DeNora cathode) is also presented in the same figure, for comparison. It is interesting to note that both electrodes possessed practically the same activity for HER at j = –0.3 A cm^{-2}.

In industrial chlor–alkali electrolysis, one of the technical methods for replacing some the electrodes by new ones is the short-circuiting of a cathode and an anode in the electrolysis bath. Then a reverse current flows through a bypass circuit and the cathode is oxidized, resulting in the loss of electrocatalytic activity for the HER. In the case of the Raney-Ni active cathode, the potential was sharply shifted in the positive potential direction immediately after the short-circuiting and reached 0.30 V *vs.* SCE within about 3 min. It was reported by Yoshida and Morimoto[22] that the reverse current on short-circuiting caused a shift of the potential toward oxidation of the Raney-Ni electrode to lower its electrocatalytic activity, due to formation of NiOOH surface oxide. In order to simulate short-circuiting condition, Ni/Ni–MoO_x cathode was repeatedly polarized at 0.30 V (SCE) for 1000 s, and polarization curves for the HER were recorded after short-circuiting (Fig. 12). At an applied current density of 300 mA cm^{-2}, a decrease of the overvoltage by about 20 mV was observed after the short-circuiting, suggesting

that the Ni/(Ni–MoO_x) active cathode kept an excellent activity irrespective of the presence and the absence of a reverse current due to short-circuiting.

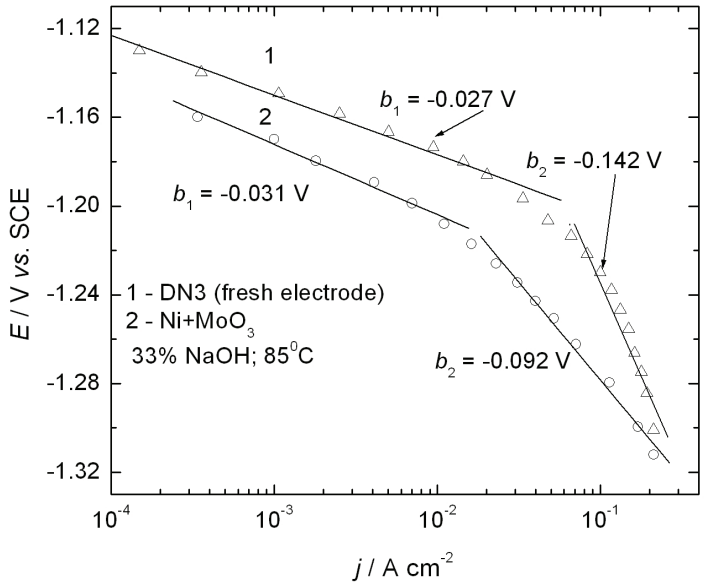

Fig. 11. Tafel polarization curves for the HER on a commercial DN3 electrode (1) and Ni/(Ni–MoO_x) electrode (2) in 33 wt. % NaOH solution at 85 °C. The composite electrode was prepared by electrodeposition from a Watt bath containing 1 g dm^{-3} of MoO_3 particles at j_{Ni} = 50 mA cm^{-2}.

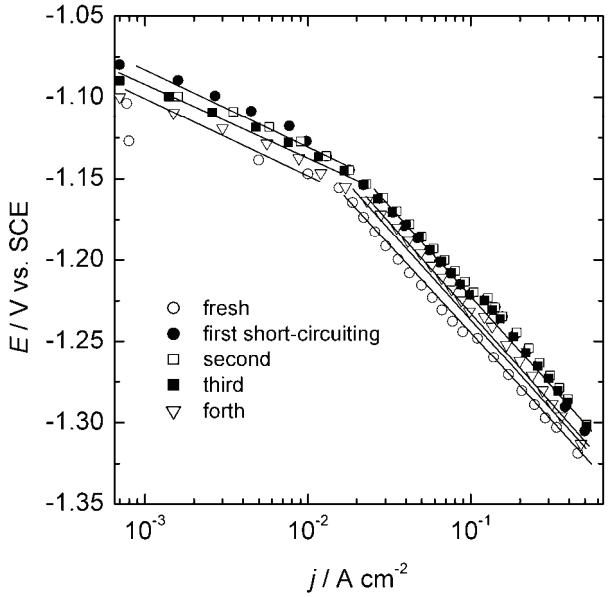

Fig. 12. Tafel polarization curves for the HER on a Ni/(Ni–MoO_x) electrode in 33 wt. % NaOH solution at 85 °C, recorded after short-circuiting. The composite electrode was prepared by electrodeposition from a Watt bath containing 1.0 g dm^{-3} of MoO_3 particles at j_{Ni} = 50 mA cm^{-2}.

CONCLUSIONS

Co-deposition of Ni and MoO_3 particles from a Watt bath produced composite catalysts that possessed high activity for the HER in strong alkaline solutions.

During co-deposition, partial reduction of the MoO_3 particles occurred and the Ni–MoO_x composite coatings prepared by deposition at lower current densities were completely amorphous in nature.

The maximum activity was obtained already at 1 g dm^{-3} MoO_3 in solution (suspension).

Co-deposition resulted in increased surface roughness. The roughness factor for the Ni–MoO_x composite electrode was two orders of magnitude higher than that of a polished Ni electrode.

The true catalytic activities of the composite Ni–NiO_x catalysts for the HER were about two orders of magnitude higher than that of an etched Ni electrode.

The Ni–MoO_x composite catalyst possessed the same activity at high current density for the HER as a commercial DeNora (DN3) electrode in 33 wt. % NaOH solution at 85 °C.

Preliminary stability tests showed that anodic pretreatment of the composite catalyst that simulated short-circuiting conditions did not deactivate the electrode for the HER.

Acknowledgment. This work is financially supported by the Ministry of Education and Science of the Republic of Serbia, under contract No. 172054.

И З В О Д

КИНЕТИКА ЕЛЕКТРОХЕМИЈСКЕ РЕАКЦИЈЕ ИЗДВАЈАЊА ВОДОНИКА НА КОМПОЗИТНИМ NI–MoO_x КАТАЛИЗАТОРИМА У АЛКАЛНИМ РАСТВОРИМА

БОРКА М. ЈОВИЋ[1], УРОШ Ч. ЛАЧЊЕВАЦ[1], ВЛАДИМИР Д. ЈОВИЋ[1], ЉИЉАНА М. ГАЈИЋ-КРСТАЈИЋ[2] и НЕДЕЉКО В. КРСТАЈИЋ[3]

[1]Институт за мултидисциплинарна истраживања, Универзитет у Београду, 11030 Београд, [2]Институт техничких наука САНУ, Кнез Михајлова 35, 11000 Београд и [3]Технолошко–металуршки факултет, Универзитет у Београду, Карнегијева 4, 11000 Београд

Композитне Ni–MoO_x превлаке су формиране истовременим таложењем никла и MoO_3 честица које су суспендоване у Watt-овом купатилу различитог састава. Морфологија и састав композитних превлака испитивани су применом цикличне волтаметрије, трансмисионе и скенирајуће електронске микроскопије и дифракцијом X-зрака. Електрокаталитичка активност композитних превлака за реакцију издвајања водоника у алкалним растворима је одређена стационарним поларизационим мерењима. Показано је да активност катализатора расте са садржајем MoO_3 у Ni превлакама до одређене граничне вредности. Композитне Ni–MoO_x превлаке испољавају високу каталитичку активност, која је слична активности комерцијалног Ni–RuO_2 (De Nora) катализатора. Тестови стабилности су показали да Ni–MoO_x катализатор задржава високу каталитичку активност при константној густини струје издвајања водоника као и одличну толеранцију према реверсној поларизацији.

(Примљено 21. јуна, ревидирано 19. септембра 2011)

REFERENCES

1. R. Parsons, *Trans. Faraday Soc*. **54** (1958) 1053
2. S. Trasatti, *J. Electroanal. Chem*. **39** (1972) 163
3. R. L. Augustine, in *Catalytic Hydrogenation*, Marcel Dekker, New York, 1985, p. 26
4. N. Elezović V. D. Jović, N. V. Krstajić, *Electrochim. Acta* **50** (2008) 5594
5. D. E. Brown, M. N. Mahmood, A. K. Turner, S. M. Hall, P. O. Fogarty, *Int. J. Hydrogen Energy* **7** (1982) 405
6. J. Y. Huot, L. Brossard, *J. Appl. Electrochem.* **18** (1988) 815
7. J. Y. Huot, L. Brossard, *J. Appl. Electrochem*. **20** (1990) 281
8. J. Y. Huot, L. Brossard, *Surf. Coat. Technol*. 34 (1998) 373
9. B. E. Conway, L. Bai, *J. Chem. Soc., Faraday Trans. 1* **81** (1985) 1841
10. M. M. Jakšić, *Mat. Chem. Phys*. **1** (1989) 22
11. M. Yoshida, Y. Noaki, in *Performance of Electrodes for Industrial Electrochemical Processes*, F. Hine, B. V. Tilak, J. M. Fenton, J. D. Lisius, Eds., The Electrochemical Society, Penington, NJ, USA, 1989, p. 15
12. L. S. Sanches, S. H. Domingues, A. Carubelli, L. H. Mascaro, *J. Braz. Chem. Soc*. **14** (2003) 556
13. L. S. Sanches, S. H. Domingues, C. B. Marino, L. H. Mascaro, *Electrochem. Commun*. **6** (2004) 543.
14. E. J. Podlaha, D. Landolt, *J. Electrochem. Soc*. **143** (1996) 893
15. E. Chassaing, N. Portail, A. F. Levy, G. Wang, *J. Appl. Electrochem*., **34** (2004)1085.
16. M. Donten, H. Cesiulis, Z. Stojek, *Electrochim. Acta* **50** (2005) 1405
17. M. Donten, H. Cesiulis, Z. Stojek, *Electrochim. Acta* **45** (2000) 3389
18. H. Cesiulis, A. Baltutiene, M. Donten, M. L. Donten, Z. Stojek, *J. Solid State Electrochem.* **6** (2002) 237
19. J. Divisek, H. Schmitz, J. Balej, *J. Appl. Electrochem*. **19** (1989) 519
20. Z. M. Hanafa, M. A. Khilla, M. H. Askae, *Thermochim. Acta* **45** (1981) 221
21. N. Krstajić, M. Popović, B. Grgur, M. Vojnović, D. Šepa, *J. Electroanal. Chem*. **512** (2001) 16
22. N. Yoshida, T. Morimoto, *Electrochim. Acta* **39** (1994) 1733.